**Preprints of the 19th World Congress**
**The International Federation of Automatic Control**
**Cape Town, South Africa. August 24-29, 2014**

# Accuracy of Stroke Volume Estimation via Reservoir Pressure Concept and Three Element Windkessel Model

**Shun Kamoi*, Dougie Squire*, James Revie*, Christopher Pretty*, Paul Docherty*, Yeong Shiong Chiew***
**Thomas Desaive**, Geoffrey M Shaw***, J. Geoffrey Chase***

**Department of Mechanical Engineering, University of Canterbury,*
*Christchurch, New Zealand (e-mail: shun.kamoi@pg.canterbury.ac.nz).*
***GIGA Cardiovascular Science, University of Liege,*
*Liege, Belgium (email: Tdesaive@ulg.ac.be)*
**** Intensive Care Unit, Christchurch Hospital,*
*Christchurch, New Zealand, (e-mail: Geoff.Shaw@cdhb.govt.nz)*

**Abstract:** Accurate stroke volume (SV) measurements can convey large amounts of information about patient hemodynamic status. However, direct measurements are too invasive in clinical practice and current procedures for estimating SV require specialised devices. This study presents an analysis of the accuracy of SV estimation by combining pulse-wave and windkessel analyses. What makes this study different to existing pulse-contour analyses is that pressure contour variation due to altered arterial mechanical properties (resistance, characteristic impedance and compliance) were related to correct corresponding pressure zones, enabling this model to more accurately capture SV from aortic pressure measurements alone.

Using data from three porcine experiments, the median difference between measured and estimated SV was 1.4 ml with a 90% range ($5^{th}$-$95^{th}$ percentile) -11.3ml - 12.2ml. This result relies on an estimate of the average value of just one windkessel parameter. The presented method demonstrates that SV can be estimated from pressure waveforms alone, without the need for identification of complex physiological metrics where strength of correlations may vary from patient to patient.

*Keywords: Biomedical systems, Physiological models, Parameter ID, Cardiovascular systems*

## 1. INTRODUCTION

Inadequate ability to diagnose cardiac dysfunction is prevalent in critical care (Franklin et al., 1994, Perkins et al., 2003) and is a significant cause of increased length of hospital stay and potential mortality (Angus et al., 2001, Brun-Buisson, 2000). However, detection, diagnosis and treatment for cardiac dysfunctions are very difficult, with clinicians confronted by large amounts of often contradictory numerical data. Thus, it is important to synthesise this raw clinical data into a readily understood physiological context to aid diagnosis and treatment.

This goal can be accomplished using computational models and patient-specific parameter identification methods to unmask hidden dynamics and interactions in measured clinical data (Taylor et al., 2009, Taylor et al., 1999). This approach can create a clearer physiological picture from the available data, making diagnosis simpler and more accurate, and enabling personalised care. In addition, this approach provides a means to monitor patients in real-time, which could enable faster diagnosis and detection of dysfunction (Kruger et al., 2011).

Ventricular stroke volume (SV) measurements are essential for evaluating cardiovascular system (CVS) function (Tibby et al., 2003, Ellender et al., 2008, Zile et al., 2002). Currently, there are many methods available for determining SV, ranging from non-invasive procedures such as ultrasound, through moderately invasive methods such as thermodilution (Alhashemi et al., 2011), to highly invasive direct measurement with admittance catheters. However, all these methods require specialised equipment and/or personnel, and often only provide intermittent values of SV or measures of average SV over long periods (cardiac output).

What is required is a means to accurately and continuously estimating SV on a beat to beat basis, or over a short time, frame that is not simply cardiac output (CO). Clinically, CO captures total flow increase whether it is due to increased heart rate (HR), or SV per beat. It is clinically important to separate these effects with an accurate SV estimation because these differences can require different therapies, but currently are not easily differentiable (Felker et al., 2001). Thus, an accurate estimate of SV would provide additional critical insight necessary for better decision making and care.

This study investigates how well continuous beat to beat SV can be estimated using only the measured aortic pressure waveform. Many other studies and devices use an arterial waveform and pulse-contour analysis to estimate SV (Marik, 2013). The unique aspect of this study is that it relates arterial mechanical properties (resistance, characteristic impedance and compliance) to the corresponding pressure zones in the

pressure waveform, enabling this model to more accurately capture SV from aortic pressure measurements alone. This study analyses the impact of fixing only one model parameter on the accuracy of the SV estimate.

## 2. METHODOLOGY

This study combines arterial windkessel behaviour (Westerhof et al., 2009) and pulse wave theory (O'Rourke et al., 2001) to estimate left-ventricular stroke volume. This approach improves estimation of SV from pressure measurements as the two are linked with improved assumptions. Figure 1 presents a schematic of the process used in this study.

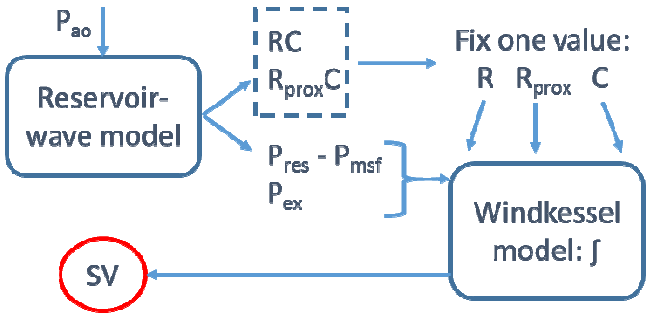


**Fig. 1**. Schematic of estimation procedure showing input, identified and estimated parameters/variables.

### *2.1 Porcine Trials and Measurements*

This study uses data from experiments performed on pigs at the centre Hospitalier Universitaire de Liege, Belgium. These experiments were primarily conducted to investigate respiratory failure, but extensive measurements of CVS variables were also recorded (van Drunen et al., 2013). All experimental procedure, protocols and the use of data in this study were reviewed and approved by the Ethics Committee of the University of Liege Medical Faculty.

Experiments were performed on three healthy, pure pietrain pigs weighing between 29 – 37kg. During the experiments, each subject underwent several step-wise positive end expiratory pressure (PEEP) recruitment manoeuvres (RM), causing changes to SV (Luecke et al., 2005). Details of the experimental procedure are published elsewhere (van Drunen et al., 2013). It should be noted that these experiment were performed with open chest. However, chest of pig 1 and 2 were held closed with forceps. Thus the SV and arterial waveform were affected by direct pressure on the mediastinum area from expanding lungs.

Left and right ventricular volumes and pressures were measured using 7F admittance catheters (Transonic Scisense Inc., Ontario, Canada) inserted directly into the ventricles through the cardiac wall. Aortic pressure was measured with a 7F pressure catheter (Transonic Scisense Inc., Ontario, Canada) inserted into the aortic arch through the carotid artery. All data were sampled at 200 Hz and were subsequently analysed using Matlab (version 2013a, The Mathworks, Natick, Massachusetts, USA).

### *2.2 Aortic Pressure Model*

The aortic pressure model used in this study is based on model proposed by Wang *et al* (2003). This model proposes that aortic pressure $P_{ao}$ can be separated into two components, reservoir pressure and excess pressure. Reservoir pressure, $P_{res}$, accounts for the energy stored/released by the elastic walls of the arterial system. Excess pressure, $P_{ex}$, is defined as the difference between the measured aortic pressure and the reservoir pressure that varies with time, ($t$). This model also describes the proportionality between the excess pressure and flow into the aortic compartment from the left ventricle ($Q_{in}$):

$$P_{ao}(t) = P_{res}(t) + P_{ex}(t) \tag{1}$$

$$P_{ex}(t) = Q_{in}(t) R_{prox} \tag{2}$$

Where $R_{prox}$ is the characteristic impedance relating inflow and excess pressure. In addition to the pressure relationships defined in Equations (1) and (2), classical three element windkessel theory was also applied (Westerhof et al., 2009), relating reservoir pressure and flow:

$$\frac{dP_{res}(t)}{dt} = \frac{Q_{in} - Q_{out}}{C} \tag{3}$$

$$\frac{P_{res}(t) - P_{msf}}{R} = Q_{out}(t) \tag{4}$$

$C$, $R$, and $P_{msf}$ are defined as compliance, resistance and mean systemic filling pressure, respectively and $Q_{out}$ is flow leaving the aortic compartment. In this case, aortic model parameters $C$, $R$, and $R_{prox}$ are assumed to be constant during single heartbeat.

By combining Equations (1) - (4), reservoir pressure can be expressed in terms of $P_{ao}$, $P_{msf}$, $R_{prox}$, $R$, and $C$:

$$\frac{dP_{res}(t)}{dt} = \frac{P_{ao}(t) - P_{res}(t)}{R_{prox} C} - \frac{P_{res}(t) - P_{msf}}{RC} \tag{5}$$

The analytical solution to Equation (5) for $P_{res}$ gives:

$$P_{res}(t) = e^{-\beta t} \cdot \left( \int_0^t e^{\beta t'} \cdot \left( \frac{P_{ao}(t')}{R_p C} + \frac{P_{msf}}{RC} \right) dt' + P_{res}(0) \right) \tag{6}$$

Where $\beta = 1/R_{prox}C + 1/RC$. Equation (6) can be used to calculate reservoir pressure, which is dependent only on three parameters $RC$, $R_{prox}C$, and $P_{msf}$.

The diastolic regions of the aortic pressure decay curve were used to identify exponential time decay constant $RC$ and $P_{msf}$. In this pressure region, inflow to the aortic compartment is assumed to be zero as a result of closure of aortic valve and that pressure decay results from only volumetric change of the arterial compartment (Aguado-Sierra et al., 2008):

$$P_{res}(t) = P_{ao}(t) \qquad (t_d \le t \le t_f) \tag{7}$$

With this assumption, Equation (5) can be reduced such that $P_{res}$ is a function of only two parameters RC and $P_{msf}$. Thus, the diastolic reservoir pressure can be expressed:

$$P_{res}(t) = (P_{ao}(t_d) - P_{msf})e^{-\frac{(t-t_d)}{RC}} + P_{msf} \quad (t_d \le t \le t_f) \quad (8)$$

Where $t_d$ and $t_f$ are the time of closure of aortic valve and total time for one cycle of heart beat, respectively. In this work, the start of diastole was defined by the time of the minimum rate of change of $P_{ao}$ (Abel, 1981).

For identification of $R_{prox}C$, the systolic pressure waveform was used along with the estimated values of $P_{msf}$ and $RC$ from the previous step. The identification of $R_{prox}C$ involves additional assumptions about the behaviour of the reservoir pressure curve. In particular, zero net flow in the compartment occurs in the region between the point of maximum $P_{ao}$ and $t_d$. Using this additional information and Equations (5) and (6), value of $P_{ao}$ is iterated in this range for the identification of $R_{prox}C$ until below condition is satisfied:

$$P_{res}(\tau) = \frac{RCP_{ao}(\tau) + R_{prox}CP_{msf}}{R_{prox}C + RC} \quad (9)$$

Where τ is the time when inflow $Q_{in}$ is equal to the outflow $Q_{out}$. Once the parameters $RC$, $R_{prox}C$, and $P_{msf}$ are estimated, $P_{ao}$ is decoupled into reservoir and excess pressure using Equations (1) and (6). Figure 2 shows approximated separated pressures and flow using identified parameters $RC$, $R_{prox}C$, and $P_{msf}$.

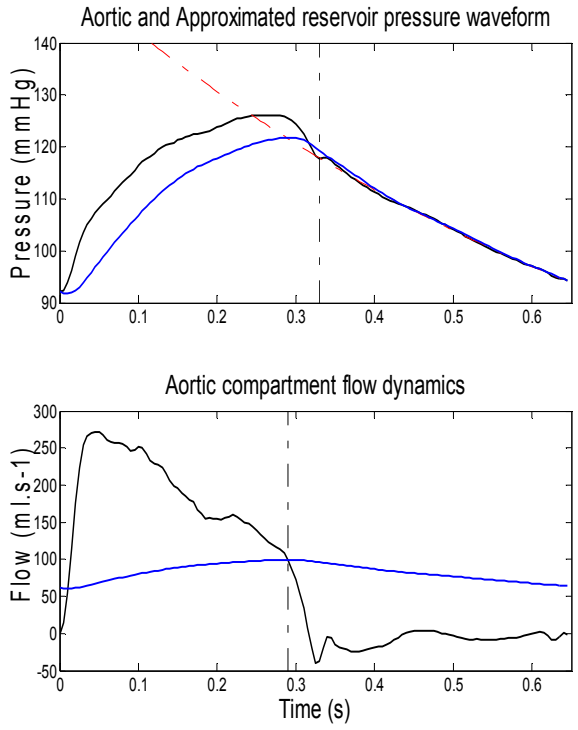


**Fig. 2** Top panel: example of aortic pressure separation showing estimated diastolic curve (red dashed line), reservoir pressure $P_{res}$ (blue line), valve closure time $t_d$ (dashed black line), and measured aortic pressure $P_{ao}$ (solid black line). Bottom panel: Estimated aortic inflow $Q_{in}$ (solid black line), outflow $Q_{out}$ (blue line), and zero net flow time τ (dashed black line.

### *2.4 Stroke Volume Estimation*

Structural identifiability analysis of this model for SV shows unique values for SV cannot be estimated unless one of the three windkessel parameters are fixed. In this analysis, experimentally measured left-ventricular SV values enable each windkessel parameter $R$, $C$, and $R_{prox}$ to be identified for each pig by minimising the error between the measured and estimated SV. By fixing one of these parameters at its optimal value, and estimating stroke volume, we can evaluate the accuracy of SV estimation from the aortic pressure waveform. Repeating this process for each 'fixed' parameter enables us to evaluate the best-case SV estimation.

Identification of each optimal, or 'fixed,' windkessel parameter was conducted by grid-search within reported physiological ranges (Hannon et al., 1990). Values of resistance, compliance, and characteristic impedance, ($R_{fixed}$, $C_{fixed}$, $R_{prox,\,fixed}$), were tested with resolution of 0.001 for each parameter:

$$[R, C, R_{prox}] = \arg\min_{[R,C,R_{prox}]} \left(\sum_{i=1}^{T_{beats}} abs\left(SV_{measured,i} - SV_{approx,i}\right)\right) \quad (10)$$

Where $T_{beats}$ is total number of heart beats for each subject. Thus, the fixed values of these parameters represent the optimal average values over all beats. Stroke volume estimation was performed using identified calibrated value of $R_{fixed}$, $C_{fixed}$, and $R_{prox,\,fixed}$ together with derived values of $P_{ex}$, $P_{res}$, $RC$, and $P_{msf}$.

$$SV_R = \frac{1}{R_{\text{fixed}}}\int_{t_0}^{t_f}(P_{res}(t) - P_{msf})dt \quad (11)$$

$$R_{C,\text{fixed}} = \frac{RC_{identified}}{C_{\text{fixed}}} \quad (12)$$

$$SV_C = \frac{1}{R_{C,\text{fixed}}}\int_{t_0}^{t_f}(P_{res}(t) - P_{msf})dt \quad (13)$$

$$SV_{R_{prox}} = \frac{1}{R_{prox,\text{fixed}}}\int_{t_0}^{t_f}P_{ex}(t)dt \quad (14)$$

Where $SV_R$, $SV_C$, and $SV_{Rprox}$, represents the estimated SV using the fixed values for resistance, compliance, and characteristic impedance, respectively. Each of the SV values represents SV estimation with only one parameter held constant within the three element windkessel ($R$, $C$, or $R_{prox}$) for the duration of the experiment.

### *2.5 Data Analysis*

The original aortic waveform data were pre-processed by removing regions where obvious measurements error occurred due to equipment or catheter disturbance or failure. Using this pre-processed data, the aortic pressure waveform was split into reservoir and excess pressure components using

the aortic model, prior to calculation of SV. In this study, agreements and distribution of differences between measured and approximated stroke volume were shown with Bland-Altman plots. In addition, zero lag cross correlation value were calculated between two waveforms, SV estimate and SV measured in the RM region where SV trend were most apparent.

## 3. RESULTS

The optimal average parameter values, $R_{fixed}$, $C_{fixed,}$ and $R_{prox,fixed}$ for each of three pigs used in this study are presented in Table 1. Bland-Altman plots for each pig are presented in Figure 3, where there are approximately 300 to 1000 estimated SV values per pig. These plots compare directly measured values of SV to values estimated using Equations (11) - (14) with values from Table 1. Table 2 and 3 summarises the results of the Bland-Altman plots and calculated zero lag cross correlation values, respectively.

**Table 1**: Optimal average parameter values in the three element windkessel model for the estimation of SV

| Pig No | $R_{fixed}$ (mmHg.s/ml) | $C_{fixed}$ (ml/mmHg) | $R_{prox,fixed}$ (mmHg.s/ml) |
|---|---|---|---|
| Pig 1 | 1.2104 | 0.6363 | 0.0825 |
| Pig 2 | 2.1353 | 0.3837 | 0.1333 |
| Pig 3 | 0.7008 | 0.9930 | 0.0395 |

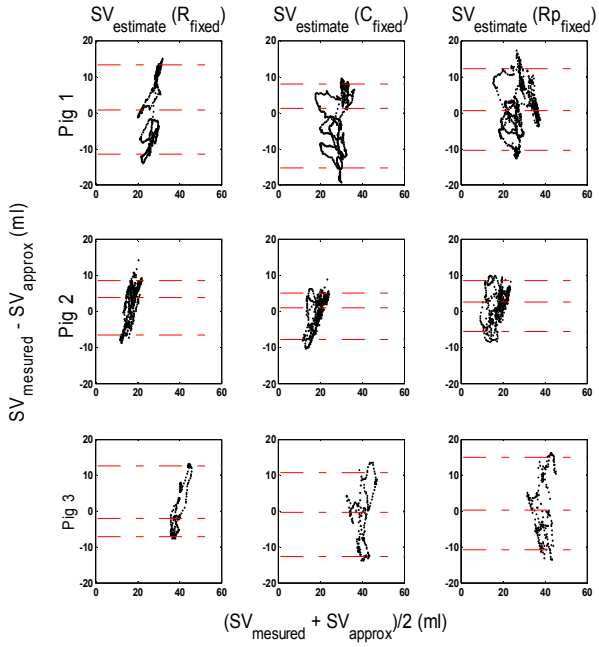


**Fig. 3**: Bland-Altman plots comparing agreements between measured and estimated SV for Pigs 1, 2 and 3 for each case of using a fixed estimate of $R$, $C$, or $R_{prox}$.

**Table 2**: Differences between estimated and measured stroke volumes calculated using different calibration parameters. Data are presented as the median [5-95$^{th}$ percentiles] from the Bland-Altman plots of Figure 2. .

| Pig No | Bland-Altman results ( ml) | | |
|---|---|---|---|
| | $\Delta SV\ R_{fixed}$ | $\Delta SV\ C_{fixed}$ | $\Delta SV\ R_{prox,fixed}$ |
| Pig 1 | 0.9 [-11.4, 13.3] | -1.1 [-15.5, 8.1] | 0.6 [-10.6, 12.3] |
| Pig 2 | 3.9 [-6.5, 8.7] | 1.0 [-7.7, 5.1] | 2.7 [-5.6, 8.6] |
| Pig 3 | -2 [-7.2, 12.5] | -0.4 [-12.8,10.8] | 0.2 [-11.0, 15.0] |
| All Pigs | 2.0 [-10.5,12.9] | 0.6 [-13.3, 8.0] | 1.5 [-9.9, 12.0] |
| Overall Average: 1.4 [-11.3, 12.2] | | | |

**Table 3**: Cross correlation coefficient between estimated and measured SV waveforms in the RM time zone

| Pig No | Zero lag cross-correlation value | | |
|---|---|---|---|
| | $R_{fixed}$ | $C_{fixed}$ | $R_{prox,fixed}$ |
| Pig 1 | 0.68 | 0.60 | 0.45 |
| Pig 2 | 0.65 | 0.86 | 0.68 |
| Pig 3 | 0.66 | 0.85 | 0.67 |

## 4. DISCUSSION

### *4.1 Optimal Parameter Values*

Table 1 shows the optimal average values for resistance, compliance and characteristic impedance for the 3 pigs. The values are noticeably different between pigs for a given calibration parameter. This result suggests the use of mean population parameters could lead to significantly different approximations and would lead to inaccurate estimation of SV if comparing across subjects. However, trends and changes would be captured, which is of clinical importance.

Figure 3, Table 2, and Table 3 demonstrate the ability for this model to capture SV. Across all beats and pigs, the median difference between measured and estimated SV was 1.4 ml, with a 90%-range of -11.3-12.2 ml. The median differences and 90%-ranges were similar for each fixed parameter. Thus, the proposed model is capable of estimating suitable SV by applying any of the three fixed parameters. It is also noted that cross correlation coefficient were in the range of 0.6 – 0.85, which suggests that SV trends due to PEEP interaction were accurately captured. This outcome allows wider application, since if any of the three parameters can be derived or estimated from additional, *a priori*, knowledge, a continuous SV estimation without external calibration (e.g. thermodilution) becomes possible.

*4.3 Stroke Volume Estimation*

Pulse contour methods have been extensively studied as a mean of estimating SV from continuous arterial blood pressure measurements (Montenij et al., 2011). However, conversions of pressure measurements to magnitude of flow are restricted to the assumptions made in the model-based approach. In particular, there are no direct relationships that can provide the scalars of volume from pressure measurements alone. As a consequence, the precision of SV estimations via model-based approaches are always limited to the assumptions made, such as strength of parameter correlations or stability of calibrated measurements (Siegel et al., 1992, Alhashemi et al., 2011).

Historically, these models have evolved and increased in complexity to capture more accurate representation of realistic physiological phenomena (Shi et al., 2011). More realistic models can provide better approximations of the SV and more detailed physiological insight. However, identification of the model parameters becomes much more difficult if not impossible, eliminating their use in practical application based patient-specific context, while increasing their use as models for understanding (Docherty et al., 2011, Raue et al., 2009).

The aortic model presented in this study incorporates pulse wave theory that is based on one dimensional flow in an elastic tube (Alastruey et al., 2009). Despite the fact that the model is a zero-dimensional cardiovascular analysis, it can be treated as one segment from a whole network of arteries represented by multiple compartments, having many zero dimensional models connected together (Parker et al., 2012). While the assumptions of this model are simplistic, they are made in consideration with what is accessible in clinical scenes (Dickstein, 2005).

Combining pulse wave theory (van de Vosse et al., 2011) and the arterial windkessel model increases the information that can be extracted from the aortic pressure contour (Thiele et al., 2011). This combination reduced the number assumptions required and allowed non-fixed parameters to be constrained within the identified parameters $RC$ and $R_{prox}C$, helping to increase the ability of the model to represent the true physiological conditions and thus estimate SV. In addition, beat-to-beat pressure contour variation due to altered arterial mechanics, $R$, $R_{prox}$, and $C$, were related to correct corresponding pressure zones, enabling this model to more accurately capture SV from aortic pressure measurements alone.

*4.4 Limitations*

The SV estimates were compared with directly measured left ventricular volumes, providing a true validation of the model accuracy to within errors using such measurements. Although left ventricular volume was measured directly and with the best available method, the sample size was small, with only 3 pigs being considered in this study. However, this study analysed over 1500 heart beats, across a range of SV values induced by changes in PEEP. The range of SV analysed covers the expected normal range for most of the pigs (Hannon et al., 1990). Thus, despite the small sample size, this study demonstrates the feasibility of accurately identifying SV using non-invasive, clinically available measurements.

In this experiment, changes to SV were induced by varying mechanical ventilation pressures, creating variation in the left ventricular preload. The effect of an increase or decrease in the thoracic cavity pressure alters the venous return to the ventricle and, as a consequence, stroke volume changes. In this study, the variations of systemic arterial mechanics are considered to be reasonably constant and the accuracy of the presented method may not be the same in the cases where the subject's hemodynamic conditions were significantly changed due severely diseased condition or extreme levels of care such as high ventilation pressures.

A further limitation of this aortic model is that the separation of aortic pressure waveform into reservoir and excess pressure represents a separation of forward and backward travelling waves. This assumption is based on the work of Wang *et al* (2003), which shows proportionality in the inflow $Q_{in}$ and excess pressure $P_{ex}$. This rationale may not hold for subjects with extraordinary or highly dysfunctional physiological conditions.

## 5. CONCLUSIONS

Physiological models are simplified representations of reality which can provide clinicians with information for decision making, without the need for additional invasive direct measurements (Massoud et al., 1998). The models presented in this study show the potential for continuous, accurate SV measurements using measurements typically available in the intensive care unit.

This method of obtaining SV from aortic pressure waveform alone is more adequate for relating our knowledge about circulatory physiology to blood pressure values. The study showed SV variations across all beats and pigs, can be captured with precision of median difference between measured and estimated SV of 1.4 ml, with a 90%-range of -11.3-12.2 ml. Moreover, the SV trends agreement showed cross correlation coefficient of above 0.6 for all cases. Thus, the aortic model is capable of estimating SV in both healthy and ARDS states with suitable accuracy.

The aortic model shows the ability for extending our current understandings of the CVS mechanics, and to optimise real-time diagnosis and cardiovascular therapy.

## REFERENCES

Abel, F. L. (1981). Maximal negative dP/dt as an indicator of end of systole. *American Journal of Physiology - Heart and Circulatory Physiology,* 240**,** 4**,** H676-H679.

Aguado-Sierra, J., Alastruey, J., Wang, J.-J., Hadjiloizou, N., Davies, J., et al. (2008). Separation of the reservoir and wave pressure and velocity from measurements at an arbitrary location in arteries. *Proceedings of the Institution of Mechanical Engineers, Part H: Journal of Engineering in Medicine,* 222**,** 4**,** 403-416.

Alastruey, J., Parker, K. H., Peiro, J. & Sherwin, S. J. (2009). Analysing the pattern of pulse waves in arterial networks: a time-domain study. *Journal of Engineering Mathematics,* 64**,** 4**,** 331-351.

Alhashemi, J. A., Cecconi, M. & Hofer, C. K. (2011). Cardiac output monitoring: an integrative perspective. *Critical Care,* 15**,** 2.

Angus, D. C., Linde-Zwirble, W. T., Lidicker, J., Clermont, G., Carcillo, J., et al. (2001). Epidemiology of severe sepsis in the United States: Analysis of incidence, outcome, and associated costs of care. *Critical Care Medicine,* 29**,** 7**,** 1303-1310.

Brun-Buisson, C. (2000). The epidemiology of the systemic inflammatory response. *Intensive Care Medicine,* 26**,** S64-S74.

Dickstein, K. (2005). Diagnosis and assessment of the heart failure patient: the cornerstone of effective management. *Eur J Heart Fail,* 7**,** 3**,** 303-8.

Docherty, P. D., Chase, J. G., Lotz, T. F. & Desaive, T. (2011). A graphical method for practical and informative identifiability analyses of physiological models: a case study of insulin kinetics and sensitivity. *Biomed Eng Online,* 10**,** 39.

Ellender, T. J. & Skinner, J. C. (2008). The use of vasopressors and inotropes in the emergency medical treatment of shock. *Emergency Medicine Clinics of North America,* 26**,** 3**,** 759-+.

Felker, G. M. & O'connor, C. (2001). Rational use of inotropic therapy in heart failure. *Current Cardiology Reports,* 3**,** 2**,** 108-113.

Franklin, C. & Mathew, J. (1994). Developing Strategies to Prevent Inhospital Cardiac-Arrest - Analyzing Responses of Physicians and Nurses in the Hours before the Event. *Critical Care Medicine,* 22**,** 2**,** 244-247.

Hannon, J. P., Bossone, C. A. & Wade, C. E. (1990). Normal Physiological Values for Conscious Pigs Used in Biomedical-Research. *Laboratory Animal Science,* 40**,** 3**,** 293-298.

Kruger, G. H. & Tremper, K. K. (2011). Advanced Integrated Real-Time Clinical Displays. *Anesthesiology Clinics,* 29**,** 3**,** 487-504.

Luecke, T. & Pelosi, P. (2005). Clinical review: Positive end-expiratory pressure and cardiac output. *Critical Care,* 9**,** 6**,** 607-21.

Marik, P. E. (2013). Noninvasive cardiac output monitors: a state-of the-art review. *J Cardiothorac Vasc Anesth,* 27**,** 1**,** 121-34.

Massoud, T. F., Hademenos, G. J., Young, W. L., Gao, E., Pile-Spellman, J., et al. (1998). Principles and philosophy of modeling in biomedical research. *The FASEB Journal,* 12**,** 3**,** 275-285.

Montenij, L. J., De Waal, E. E. C. & Buhre, W. F. (2011). Arterial waveform analysis in anesthesia and critical care. *Current Opinion in Anesthesiology,* 24**,** 6**,** 651-656.

O'rourke, M. F., Pauca, A. & Jiang, X. J. (2001). Pulse wave analysis. *Br J Clin Pharmacol,* 51**,** 6**,** 507-22.

Parker, K., Alastruey, J. & Stan, G.-B. (2012). Arterial reservoir-excess pressure and ventricular work. *Medical & Biological Engineering & Computing,* 50**,** 4**,** 419-424.

Perkins, G. D., Mcauley, D. F., Davies, S. & Gao, F. (2003). Discrepancies between clinical and postmortem diagnoses in critically ill patients: an observational study. *Critical Care,* 7**,** 6**,** R129-R132.

Raue, A., Kreutz, C., Maiwald, T., Bachmann, J., Schilling, M., et al. (2009). Structural and practical identifiability analysis of partially observed dynamical models by exploiting the profile likelihood. *Bioinformatics,* 25**,** 15**,** 1923-9.

Shi, Y., Lawford, P. & Hose, R. (2011). Review of Zero-D and 1-D Models of Blood Flow in the Cardiovascular System. *BioMedical Engineering OnLine,* 10**,** 1**,** 33.

Siegel, L. C. & Pearl, R. G. (1992). Noninvasive Cardiac-Output Measurement - Troubled Technologies and Troubled Studies. *Anesthesia and Analgesia,* 74**,** 6**,** 790-792.

Taylor, C. A., Draney, M. T., Ku, J. P., Parker, D., Steele, B. N., et al. (1999). Predictive medicine: computational techniques in therapeutic decision-making. *Comput Aided Surg,* 4**,** 5**,** 231-47.

Taylor, C. A. & Figueroa, C. A. (2009). Patient-Specific Modeling of Cardiovascular Mechanics. *Annual Review of Biomedical Engineering,* 11**,** 109-134.

Thiele, R. H. & Durieux, M. E. (2011). Arterial Waveform Analysis for the Anesthesiologist: Past, Present, and Future Concepts. *Anesthesia and Analgesia,* 113**,** 4**,** 766-776.

Tibby, S. M. & Murdoch, I. A. (2003). Monitoring cardiac function in intensive care. *Archives of Disease in Childhood,* 88**,** 1**,** 46-52.

Van De Vosse, F. N. & Stergiopulos, N. (2011). Pulse Wave Propagation in the Arterial Tree. *Annual Review of Fluid Mechanics, Vol 43,* 43**,** 467-499.

Van Drunen, E. J., Chiew, Y. S., Zhao, Z., Lambermont, B., Janssen, N., et al. (2013). Visualisation of Time-Variant Respiratory System Elastance in ARDS Models. *Biomed Tech (Berl)*.

Wang, J.-J., O'brien, A. B., Shrive, N. G., Parker, K. H. & Tyberg, J. V. (2003). Time-domain representation of ventricular-arterial coupling as a windkessel and wave system. *American Journal of Physiology - Heart and Circulatory Physiology,* 284**,** 4**,** H1358-H1368.

Westerhof, N., Lankhaar, J. W. & Westerhof, B. E. (2009). The arterial Windkessel. *Medical & Biological Engineering & Computing,* 47**,** 2**,** 131-141.

Zile, M. R. & Brutsaert, D. L. (2002). New concepts in diastolic dysfunction and diastolic heart failure: Part I Diagnosis, prognosis, and measurements of diastolic function. *Circulation,* 105**,** 11**,** 1387-1393.